

Frustrated Quantum Magnetism on Complex Networks: What Sets the Total Spin

G Preethi¹ and Shovan Dutta²

¹*School of Physics, IISER Thiruvananthapuram, Kerala 695551, India*

²*Raman Research Institute, Bangalore 560080, India*

(Dated: March 22, 2024)

Consider equal antiferromagnetic Heisenberg interactions between qubits sitting at the nodes of a complex, nonbipartite network. We ask the question: How does the network topology determine the net magnetization of the ground state and to what extent is it tunable? By examining various network families with tunable properties, we demonstrate that (i) graph heterogeneity, i.e., spread in the number of neighbors, is essential for a nonzero total spin, and (ii) other than the average number of neighbors, the key structure governing the total spin is the presence of (disassortative) hubs, as opposed to the level of frustration. We also show how to construct simple networks where the magnetization can be tuned over its entire range across both abrupt and continuous transitions, which may be realizable on existing platforms. Our findings pose a number of fundamental questions and strongly motivate wider exploration of quantum many-body phenomena beyond regular lattices.

Understanding how a network of pairwise interactions between dynamical units control their collective behavior is a unifying challenge for modern science. While condensed matter physics has traditionally focused on short-range interactions on a lattice, the multidisciplinary field of complex networks [1–3] has shown, over the past few decades, that the network topology itself can play a pivotal role [4]. In particular, structures not found in regular lattices, e.g., heterogeneity in the number of neighbors, the small-world effect [5], dissimilarity between adjacent nodes [6], and communities [7], can radically alter critical phenomena, disease spreading, synchronization, response to node failures, and other dynamical processes [4, 8–12].

However, most of these findings are for classical systems. While there is a sizable literature on single-particle quantum dynamics [13–17] and quantum communication networks [16, 17], the exploration of quantum *many-body* networks is in its infancy [16]. A few isolated studies have found a strong impact of heterogeneity [18, 19] and an absence of small-world effect [20] in certain quantum phase transitions, faster information scrambling with sparse long-range bonds [21, 22], and an insensitivity to graph topology in the effect of local measurements [23]. However, there is no general understanding of how the network structure governs collective quantum phenomena, especially in frustrated systems. The question is not just of fundamental interest but also timely, as it would soon be possible to engineer arbitrary interaction graphs between qubits with long coherence times, most notably with trapped ions [24–27] and superconducting circuits [28–32], among other platforms [33–38].

In the context of magnetism, networks can encode variable levels of geometric frustration, which is at the heart of exotic phases of matter such as spin liquids [39, 40]. Frustration arises whenever all bonds cannot be simultaneously satisfied, the simplest example being a triangle with antiferromagnetic bonds [41]. Studies of frustration in (undirected) complex networks have focused on social imbalance [42] and classical Ising spin-glass physics [8].

In contrast, we consider an antiferromagnetic Heisenberg model of qubits, $\hat{H} = \sum_{i,j} J_{i,j} \hat{\mathbf{S}}_i \cdot \hat{\mathbf{S}}_j$, where we usually take $J_{i,j} = J > 0$ on all bonds to focus on the role of network topology as opposed to bond disorder. For a bipartite graph the ground state is obtained by oppositely aligning the two sublattices (of size N_A and N_B), yielding a total spin $S_{\text{total}} = |N_A - N_B|/2$ [43]. On the other hand, for a nonbipartite lattice (e.g., Kagome) frustration can stabilize a quantum spin liquid composed of fluctuating singlets with $S_{\text{total}} = 0$ but no conventional long-range order [44–46]. Here we explore what sets S_{total} in a complex nonbipartite graph and to what extent it is tunable. Although far from characterizing the ground state, our findings reveal surprising ways in which network topology shapes collective behavior of such systems.

We study a variety of networks in which key structural properties such as heterogeneity, number of triangles, average degree (number of neighbors), degree-degree correlations, and average path length between two nodes can be varied independently. We present the S_{total} distribution over thousands of graphs with $N = 30$ qubits using matrix product states [47] in the ITensor library [48] with a singular-value cutoff of 10^{-14} and a maximum bond dimension of 5000, for which almost all graphs converged to an integer total spin. The same statistical features are obtained from exact diagonalization for $N = 20$. Our results show, in particular, that S_{total} is not sensitive to the level of frustration. Instead, it can be tuned over almost its entire range by embedding “hubs” connected to many low-degree nodes in a wider network, which can be understood intuitively. These findings constrain the ground-state magnetic order and raise open questions on the wider role of frustration.

Random graphs.—We start by examining (connected) random graphs of N spins with N_e bonds. Figure 1(a) shows the distribution of S_{total} over an ensemble of such networks. We notice that S_{total} is small compared to its upper bound, $S_{\text{max}} = N/2$, which one might expect considering we have antiferromagnetic coupling on all bonds.

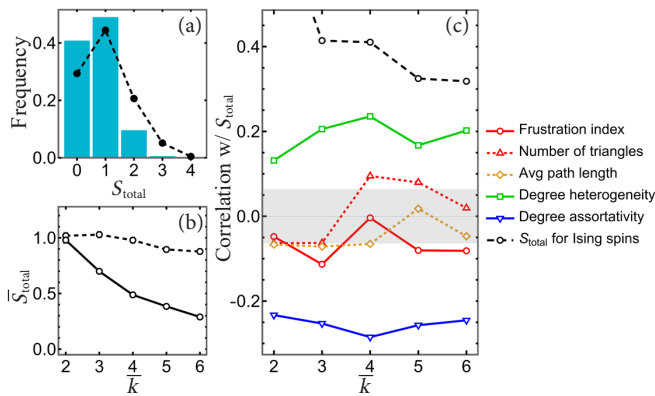


FIG. 1. (a) Bars show the distribution of total spin in the ground state of $\mathcal{N} = 916$ random graphs with $N = 30$ qubits and $N_e = 45$ bonds with equal antiferromagnetic Heisenberg coupling. The dashed curve shows S_{total} for Ising spins. (b) Ensemble average of S_{total} vs average degree $\bar{k} = 2N_e/N$ with $\mathcal{N} \approx 924$. (c) Correlation with various graph metrics. Points inside the gray band are statistically insignificant.

Second, as shown in Fig. 1(b), the average magnetization \bar{S}_{total} falls monotonically with N_e or, equivalently, the average degree $\bar{k} = \frac{2N_e}{N}$. This trend is consistent across all families of networks that we study, and it interpolates between known limiting cases: For $N_e^{\text{min}} = N - 1$ one gets a random tree where a sublattice imbalance $|N_A - N_B|$ can give rise to a net magnetization, with $\bar{S}_{\text{total}} \approx 0.23\sqrt{N}$ (see Supplement [49]). Conversely, $N_e^{\text{max}} = N(N - 1)/2$ gives an all-to-all graph, where $\hat{H} = \frac{1}{2}\hat{S}_{\text{total}}^2$ up to a constant and the ground state has $S_{\text{total}} = 0$.

More importantly, Fig. 1(c) shows that S_{total} is not sensitive to the frustration level of a graph but rather to its heterogeneity and assortativity [6]. We look at three measures of frustration [50]: (1) the frustration index N_f , which is the minimum number of bonds one needs to cut to make the graph bipartite [50–52], (2) the number of triangles, which is a more local measure, and (3) the average path length (number of hops) between two nodes, which controls how strongly a given spin can affect any other spin in the network, adding to the level of frustration. Surprisingly, we find that all three measures have weak or no correlation with S_{total} . Instead, S_{total} is correlated with the amount of heterogeneity and assortativity: The former is quantified by Δk , the spread in the number of neighbors across the network [4], whereas the latter keeps track of degree-degree correlation, i.e., whether high-degree nodes connect to high-degree nodes ($A > 0$) or to low-degree nodes ($A < 0$) [6]. Figure 1(c) tells us that the magnetization is larger for more heterogeneous graphs where high-degree nodes link to low-degree nodes. Below we systematically vary these structural properties in turn to make sense of the correlations.

The strongest correlation seen in Fig. 1(c) is with the total spin for (classical) Ising spins on the same network.

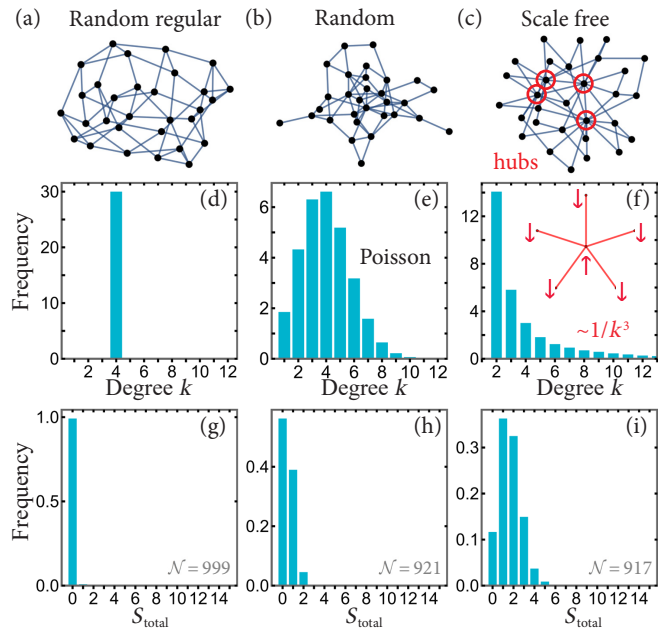


FIG. 2. Sample graph (top), degree distribution (middle), and S_{total} distribution (bottom) for random regular, random, and scale-free Barabási-Albert networks with $N = 30$ and $\bar{k} \approx 4$. The power-law tail in (f) gives rise to hubs [circled in (c)] that want to polarize their neighborhoods, as shown in the inset.

The latter is given by an optimal bipartition (also known as the max-cut problem [8, 51]), where one divides the spins into two oppositely aligned groups A and B so as to maximize the number of A - B bonds. As shown in Fig. 1, this bipolar state overestimates S_{total} for the Heisenberg spins, especially at larger \bar{k} . Nonetheless, it is useful for interpreting some of the results.

Importance of heterogeneity.—Suppressing heterogeneity results in the family of random regular graphs, where each spin has the same degree k . Figure 2(g) shows that for $k = 3$ one almost always (more than 98% of the cases) has $S_{\text{total}} = 0$, and the same holds for $k > 3$ (see Supplement [49]). This strong result shows that heterogeneity is essential for a nonzero total spin. Conversely, one can ramp up the heterogeneity by producing scale-free graphs [53] where the degree distribution p_k follows a power law. A well known example is the Barabási-Albert model [54], for which $p_k \sim 1/k^3$. As shown in Fig. 2(i), these graphs exhibit much higher magnetizations. The enhancement can be understood as originating from “hubs,” i.e., nodes with a disproportionately high degree. Such hubs form a locally star structure, favoring a net spin imbalance [see Fig. 2(f) inset]. As we discuss below, this effect persists when hubs are embedded in a broader class of networks.

Insensitivity to frustration.—An alternative argument for the unmagnetized nature of random regular graphs [Fig. 2(g)] could be that they have fewer short loops compared to random graphs [55, 56], so they appear locally treelike. Thus, S_{total} is small due to lack of frustration,

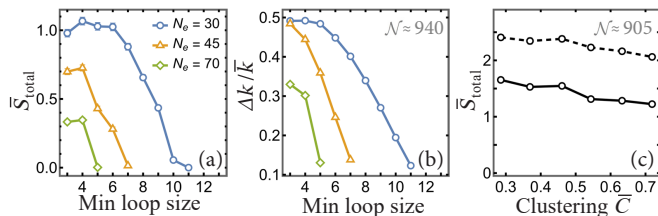


FIG. 3. (a) Average total spin and (b) heterogeneity, given by the standard deviation Δk of the degree distribution, for random graphs without short loops and $N = 30$. (c) \bar{S}_{total} for Barabási-Albert graphs with $N = 30$, $\bar{k} = 3.8$, and tunable number of triangles, measured by the mean clustering coefficient $C \in [0, 1]$ [5]. Dashed curve shows \bar{S}_{total} for Ising spins.

not because of homogeneity. To test this proposition, we directly vary the number of short loops in two different ways and see its effect on S_{total} : First, we uniformly sample from random graphs without loops of up to a given size l [57]. We find that the total-spin distribution is almost unaffected by removing all triangles ($l = 3$). As l is increased further, \bar{S}_{total} eventually drops to zero at some threshold $l = l_c$ [Fig. 3(a)]; however, l_c depends strongly on the number of bonds N_e and \bar{S}_{total} does not appear to be sensitive as to whether l is even or odd. Instead, it follows the variation in the degree distribution, which becomes progressively narrower with the removal of short loops [Fig. 3(b)]. Thus, we infer that S_{total} is dictated by the heterogeneity and not by the frustration. Second, we follow Ref. [58] to augment the Barabási-Albert model with a triangle formation step, which allows one to tune the number of triangles without changing the degree distribution or the assortativity. As shown in Fig. 3(c), this yields a weak variation of \bar{S}_{total} which is reproduced by the optimal bipartition. We also find that \bar{S}_{total} does not vary appreciably with shorter path lengths in small-world graphs (see Supplement [49]).

While this indifference to frustration may be counterintuitive, note the same holds on lattices, where both non-frustrated (e.g., square) and frustrated (e.g., Kagome) cases have $S_{\text{total}} = 0$, albeit with very different magnetic order. Likewise, we expect frustration to be important in setting the order on general networks.

Importance of disassortativity.—Not all heterogeneous networks have large magnetization. Another key metric is the assortativity coefficient $A \in [-1, 1]$ [6]. Perfect assortativity ($A = 1$) requires all nodes to have the same degree (for which $S_{\text{total}} \simeq 0$), whereas perfect disassortativity ($A = -1$) occurs in a star graph and, more generally, in complete bipartite graphs with sublattice imbalance [59] (where S_{total} can be large). Crucially, one can tune A without altering the degrees via rewiring pairs of bonds [60, 61] or by solving a linear optimization problem [59]. Thus, Figs. 4(a) and 4(b) show two graphs with very different values of A but the same degrees (hence, the same heterogeneity). The first graph is the most dis-

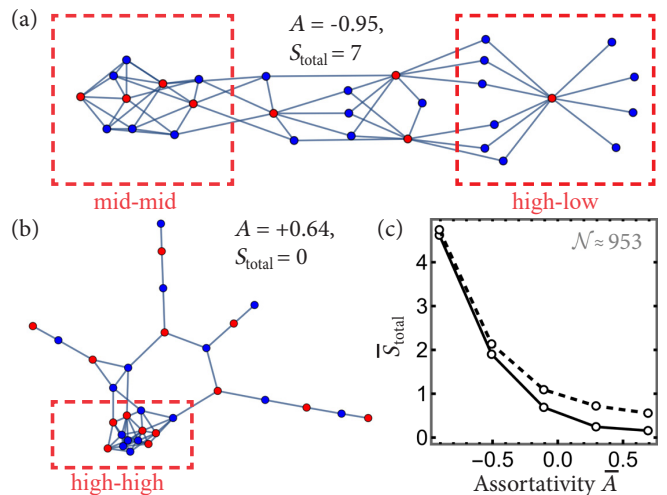


FIG. 4. (a) Most disassortative and (b) most assortative networks with the same degree sequence. Node colors show a bipolar ground state of Ising spins. (c) Variation of \bar{S}_{total} as the assortativity [6] is tuned for random graphs with $N = 30$ and $\bar{k} = 4$. Dashed curve shows the variation for Ising spins.

assortative and has $S_{\text{total}} = 7$, whereas the latter is the most assortative and has $S_{\text{total}} = 0$. The physical origin of this large disparity becomes clear if one examines the structure of these networks [60]: Strongly disassortative graphs have a section where few high-degree nodes (hubs) connect to many low-degree nodes in an approximately bipartite structure [Fig. 4(a)], which gives rise to a large spin imbalance. By contrast, in strongly assortative graphs high-degree nodes form a tightly connected group and low-degree nodes form a treelike structure [Fig. 4(b)], neither of which favors a large magnetization. Note that the large S_{total} in the former case requires both the presence of hubs and disassortativity.

Figure 4(c) shows that \bar{S}_{total} falls sharply as we tune A from its minimum to maximum value for random graphs. The same behavior is observed for Ising spins and for scale-free graphs (see Supplement [49]).

Tunable spin distribution.—Fortunately, we can use a simple model to grow networks with tunable heterogeneity and assortativity. It has a parameter $m \in \mathbb{Z}$ that sets the average degree and another parameter $p \in [0, 1]$ that controls the structure. The protocol starts with a small clique of m nodes, and in each step links a new node i to m existing nodes as follows: (1) Select an existing node j at random, (2) with probability p link (i, j) , (3) else link i to a neighbor of j with preferential attachment, i.e., with probability proportional to the neighbor’s degree. This is a variant of the “copy models” for the Web [62–64].

As shown in Fig. 5(a), for $p = 0$ we get strongly disassortative graphs where many low-degree “outer” nodes connect to a few “central” hubs. As p is increased to 1, the graphs become more homogeneous [Fig. 5(b)]. Thus, both the heterogeneity and the disassortativity fall mono-

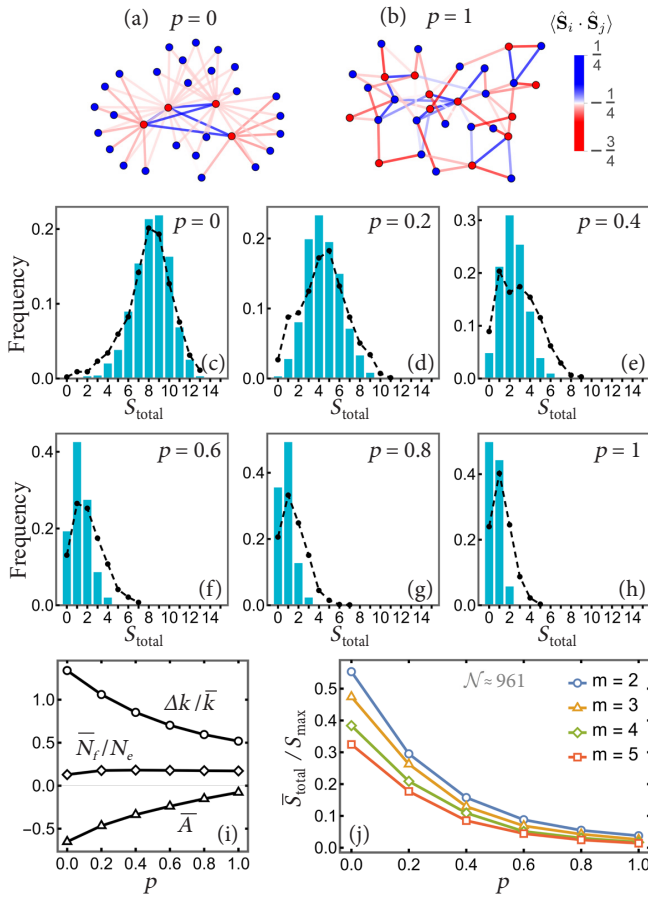


FIG. 5. (a) Graph with embedded hubs and (b) graph with no hubs generated by the growth model described in text. Node colors show the ground state for Ising spins and bond colors show ground-state correlations for our Heisenberg model. (c)–(f) Variation of the total-spin distribution with the structure parameter p for $N = 30$ and $\bar{k} = 3.8$. Dashed curves are for Ising spins. (i) Corresponding variation of heterogeneity Δk , frustration index N_f , and assortativity A . (j) Average total spin as a function of p and $\bar{k} = 2m - m(m+1)/N$ for $N = 30$.

tonically with p , while the frustration level varies weakly, as in Fig. 5(i). Accordingly, we find that the total-spin distribution is peaked at a macroscopic value of $O(N)$ for $p = 0$ and moves toward zero as p goes to 1 [Figs. 5(c)–5(h)]. In addition, \bar{S}_{total} decreases with the average degree $\bar{k} \approx 2m$ [Fig. 5(j)] as in random graphs.

In Fig. 5(c) the distribution is broad, covering almost the full range of S_{total} . Here, the maximum total spin occurs when all of the outer nodes link to the initial clique, producing a star configuration with m giant central hubs [as in Fig. 6(a) without the outer ring]. For $N \gg m$ it is then energetically favorable to align the hub spins opposite to the outer spins, which gives $S_{\text{total}} = N/2 - m$. However, during the growth stage a new node may connect to an outer node instead, which can then accumulate more bonds to become a mini hub, at the expense the initial clique which now has fewer bonds. In other words,

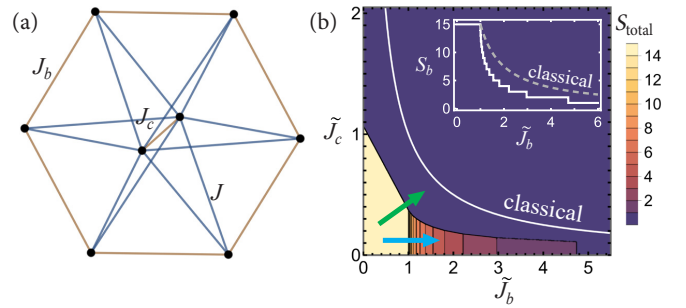


FIG. 6. (a) Wheel graph with 2 central spins and $N_b = 6$ outer spins. (b) Phase diagram for $N_b = 30$ and rescaled couplings $\tilde{J}_b := 4J_b/(JN_c)$ and $\tilde{J}_c := J_c N_c/(JN_b)$. Green arrow shows a discontinuous transition from a state where central and outer spins are oppositely aligned to a state where both add up to zero. Blue arrow shows a continuous transition where the net outer spin S_b falls in steps of 1 at a rate $\sim N_b(\tilde{J}_b - 1)^{-1/2}$ (inset). This divergence is absent for classical Heisenberg spins (dashed curve), for which $S_{\text{total}} = 0$ for $\tilde{J}_b \tilde{J}_c > 1$ (solid curve).

the giant hubs can break into several smaller hubs, which then align opposite to the outer nodes [see Fig. 5(a)], reducing S_{total} . Note that the bonds between the hubs add frustration but do not change the total spin.

Tuning S_{total} in a non-random frustrated network.— Motivated by these results, we propose a simple wheel geometry where one can deterministically vary S_{total} across its range by tuning some of the bond strengths, which may be easier to implement experimentally. The wheel consists of N_c central spins with all-to-all coupling J_c , N_b outer spins forming a ring with coupling J_b , and all bonds between the two sets of strength J , forming the spokes. Figure 6(a) shows a sketch for $N_c = 2$ and $N_b = 6$.

To understand its behavior, note that the spokes favor both the outer spin S_b and the central spin S_c to be large but anti-aligned, i.e., $S_{\text{total}} = |S_b - S_c|$, whereas J_b and J_c want to suppress S_b and S_c , respectively. For simplicity, let us consider $N_c = 2$ and N_b even. Then the central spins form either a singlet or a triplet, depending on how strongly the central bonds compete with the spokes. For $J_c N_c^2 \gg JN_b N_c$ we expect $S_c = 0$, which reduces the network to just the ring, yielding $S_b = 0$ and $S_{\text{total}} = 0$. In contrast, for $J_c N_c^2 \ll JN_b N_c$ we expect $S_c = 1$, which leads to a competition between the spokes and the outer bonds: For $J_b N_b \ll JN_b N_c$ the outer spins align, so that $S_b = N_b/2$ and $S_{\text{total}} = N_b/2 - 1$, whereas for $J_b N_b \gg JN_b N_c$ they cancel, giving $S_b = 0$ and $S_{\text{total}} = 1$. Thus, by varying J_b and J_c one should be able to stabilize any total spin between 0 and $N_b/2 - 1$.

These intuitions are confirmed by solving the system exactly using the Bethe Ansatz solution for the Heisenberg ring [65, 66] (see Supplement [49] for details). For $N_c = 2$ this gives the phase diagram in Fig. 6(b). As expected, we find an extended antiferromagnetic region where $S_b = S_c = 0$ and an extended ferromagnetic region

where both spins are maximum but oppositely aligned. The two regions share a border where the magnetization collapses abruptly (green arrow). On the other hand, for small J_c the outer spin falls in steps of 1 with J_b , exhibiting a power-law diverging susceptibility at $J_b = JN_c/4$. Interestingly, this blow up is absent for classical Heisenberg spins (see Supplement [49]), for which S_{total} is generally higher. For odd N_c the center cannot form a singlet, so there is always a competition between J and J_b , leading to a stepwise decrease of S_{total} (see Supplement [49] for the phase diagram for $N_c = 3$).

Outlook.—Perhaps the most promising platform for realizing our setup is ion traps, for which there are concrete protocols for engineering arbitrary pairwise Heisenberg coupling with existing technology for several tens of qubits [25–27]. A large class of networks can also be fabricated in photonic platforms [29, 30], where Heisenberg interactions may be simulated digitally [28, 35] or using tailored light-matter coupling [67]. Our results support the general view that hubs promote cohesion across a network [4] (e.g., ferromagnetic ordering [8, 68–70]), while pointing out the importance of assortativity [6, 71].

At the same time, they raise a number of open questions: (1) Why is S_{total} insensitive to frustration? This is far from obvious and likely depends on the mechanism for magnetic interactions. In fact, preliminary calculations show that frustration strongly affects S_{total} when magnetism arises from the delocalization of a doped carrier [72, 73]. (2) A related and perhaps the most crucial question concerns the nature of the ground state. Studies of classical Ising spins have found a glassy phase on small-world and scale-free networks [8, 74–76]. Are quantum fluctuations in the Heisenberg model strong enough to stabilize a spin liquid in the absence of a lattice symmetry [77]? (3) What are the dynamical and ergodicity properties and how are these affected by the network topology? (4) Is the magnetic order sensitive to motifs [78] other than hubs, or to community structures that regulate cooperative phenomena such as synchronization [71]? The latter arises in cluster magnetism [79]. (5) How does the physics change with bond disorder [8] or anisotropy? (6) As natural interactions decay with distance, it is useful to model spatial networks [9], which may be designed with Rydberg atoms in tweezers [80, 81]. Finally, we hope our findings herald broader explorations of quantum many-body networks beyond frustrated magnetism.

We thank Sitabhra Sinha and Sthitadhi Roy for useful discussions and comments. SD acknowledges use of the HPC facility at MPIPKS, Dresden.

[1] S. H. Strogatz, Exploring complex networks, *Nature (London)* **410**, 268 (2001).
 [2] M. E. J. Newman, *Networks: An Introduction* (Oxford

University Press, Oxford, UK, 2018).
 [3] A. S. da Mata, Complex networks: a mini-review, *Braz. J. Phys.* **50**, 658 (2020).
 [4] A. Barrat, M. Barthelemy, and A. Vespignani, *Dynamical Processes on Complex Networks* (Cambridge University Press, Cambridge, UK, 2008).
 [5] D. J. Watts and S. H. Strogatz, Collective dynamics of ‘small-world’ networks, *Nature (London)* **393**, 440 (1998).
 [6] M. E. J. Newman, Assortative mixing in networks, *Phys. Rev. Lett.* **89**, 208701 (2002).
 [7] M. E. J. Newman, Communities, modules and large-scale structure in networks, *Nat. Phys.* **8**, 25 (2011).
 [8] S. N. Dorogovtsev, A. V. Goltsev, and J. F. F. Mendes, Critical phenomena in complex networks, *Rev. Mod. Phys.* **80**, 1275 (2008).
 [9] S. Boccaletti, V. Latora, Y. Moreno, M. Chavez, and D. Hwang, Complex networks: Structure and dynamics, *Phys. Rep.* **424**, 175 (2006).
 [10] R. Albert and A.-L. Barabási, Statistical mechanics of complex networks, *Rev. Mod. Phys.* **74**, 47 (2002).
 [11] R. M. D’Souza, J. Gómez-Gardeñes, J. Nagler, and A. Arenas, Explosive phenomena in complex networks, *Adv. Phys.* **68**, 123 (2019).
 [12] S. Boccaletti, J. A. Almendral, S. Guan, I. Leyva, Z. Liu, I. Sendiña Nadal, Z. Wang, and Y. Zou, Explosive transitions in complex networks’ structure and dynamics: Percolation and synchronization, *Phys. Rep.* **660**, 1 (2016).
 [13] O. Mülken and A. Blumen, Continuous-time quantum walks: Models for coherent transport on complex networks, *Phys. Rep.* **502**, 37 (2011).
 [14] R. Berkovits, Localisation of optical modes in complex networks, *Eur. Phys. J. Special Topics* **161**, 259 (2008).
 [15] K. S. Tikhonov and A. D. Mirlin, From Anderson localization on random regular graphs to many-body localization, *Ann. Phys. (Amsterdam)* **435**, 168525 (2021).
 [16] J. Nokkala, J. Piilo, and G. Bianconi, Complex quantum networks: a topical review, [arXiv:2311.16265](https://arxiv.org/abs/2311.16265) (2023).
 [17] J. Biamonte, M. Faccin, and M. De Domenico, Complex networks from classical to quantum, *Commun. Phys.* **2**, 53 (2019).
 [18] A. Halu, L. Ferretti, A. Vezzani, and G. Bianconi, Phase diagram of the Bose-Hubbard model on complex networks, *Europhys. Lett.* **99**, 18001 (2012).
 [19] A. Halu, S. Garnerone, A. Vezzani, and G. Bianconi, Phase transition of light on complex quantum networks, *Phys. Rev. E* **87**, 022104 (2013).
 [20] M. Ostilli, Absence of small-world effects at the quantum level and stability of the quantum critical point, *Phys. Rev. E* **102**, 052126 (2020).
 [21] G. Bentsen, T. Hashizume, A. S. Buyskikh, E. J. Davis, A. J. Daley, S. S. Gubser, and M. Schleier-Smith, Treelike interactions and fast scrambling with cold atoms, *Phys. Rev. Lett.* **123**, 130601 (2019).
 [22] J.-G. Hartmann, J. Murugan, and J. P. Shock, Chaos and scrambling in quantum small worlds, [arXiv:1901.04561](https://arxiv.org/abs/1901.04561) (2019).
 [23] B. Sundar, M. Walschaers, V. Parigi, and L. D. Carr, Response of quantum spin networks to attacks, *J. Phys. Complex.* **2**, 035008 (2021).
 [24] C. Monroe, W. C. Campbell, L.-M. Duan, Z.-X. Gong, A. V. Gorshkov, P. W. Hess, R. Islam, K. Kim, N. M. Linke, G. Pagano, P. Richerme, C. Senko, and N. Y. Yao, Programmable quantum simulations of spin systems with

- trapped ions, *Rev. Mod. Phys.* **93**, 025001 (2021).
- [25] S. Korenblit, D. Kafri, W. C. Campbell, R. Islam, E. E. Edwards, Z.-X. Gong, G.-D. Lin, L.-M. Duan, J. Kim, K. Kim, and C. Monroe, Quantum simulation of spin models on an arbitrary lattice with trapped ions, *New J. Phys.* **14**, 095024 (2012).
- [26] Y. H. Teoh, M. Drygala, R. G. Melko, and R. Islam, Machine learning design of a trapped-ion quantum spin simulator, *Quantum Sci. Tech.* **5**, 024001 (2020).
- [27] Z. Davoudi, M. Hafezi, C. Monroe, G. Pagano, A. Seif, and A. Shaw, Towards analog quantum simulations of lattice gauge theories with trapped ions, *Phys. Rev. Res.* **2**, 023015 (2020).
- [28] L. Lamata, A. Parra-Rodriguez, M. Sanz, and E. Solano, Digital-analog quantum simulations with superconducting circuits, *Adv. Phys. X* **3**, 1457981 (2018).
- [29] D. I. Tsomokos, S. Ashhab, and F. Nori, Using superconducting qubit circuits to engineer exotic lattice systems, *Phys. Rev. A* **82**, 052311 (2010).
- [30] A. J. Kollár, M. Fitzpatrick, P. Sarnak, and A. A. Houck, Line-graph lattices: Euclidean and non-Euclidean flat bands, and implementations in circuit quantum electrodynamics, *Commun. Math. Phys.* **376**, 1909 (2019).
- [31] T. Onodera, E. Ng, and P. L. McMahon, A quantum annealer with fully programmable all-to-all coupling via Floquet engineering, *npj Quantum Inf.* **6**, 48 (2020).
- [32] A. D. King *et al.*, Quantum critical dynamics in a 5,000-qubit programmable spin glass, *Nature* **617**, 61 (2023).
- [33] W. Lechner, P. Hauke, and P. Zoller, A quantum annealing architecture with all-to-all connectivity from local interactions, *Sci. Adv.* **1**, e1500838 (2015).
- [34] X. Qiu, P. Zoller, and X. Li, Programmable quantum annealing architectures with Ising quantum wires, *PRX Quantum* **1**, 020311 (2020).
- [35] C.-L. Hung, A. González-Tudela, J. I. Cirac, and H. J. Kimble, Quantum spin dynamics with pairwise-tunable, long-range interactions, *Proc. Natl. Acad. Sci. U.S.A.* **113**, E4946 (2016).
- [36] P. L. McMahon, A. Marandi, Y. Haribara, R. Hamerly, C. Langrock, S. Tamate, T. Inagaki, H. Takesue, S. Utsunomiya, K. Aihara, R. L. Byer, M. M. Fejer, H. Mabuchi, and Y. Yamamoto, A fully programmable 100-spin coherent ising machine with all-to-all connections, *Science* **354**, 614 (2016).
- [37] F. Fung, E. Rosenfeld, J. D. Schaefer, A. Kabcenell, J. Gieseler, T. X. Zhou, T. Madhavan, N. Aslam, A. Yacoby, and M. D. Lukin, Programmable quantum processors based on spin qubits with mechanically-mediated interactions and transport, *arXiv:2307.12193* (2023).
- [38] L. Schlipf, T. Oeckinghaus, K. Xu, D. B. R. Dasari, A. Zappe, F. F. de Oliveira, B. Kern, M. Azarkh, M. Drescher, M. Ternes, K. Kern, J. Wrachtrup, and A. Finkler, A molecular quantum spin network controlled by a single qubit, *Sci. Adv.* **3**, e1701116 (2017).
- [39] C. Lacroix, P. Mendels, and F. Mila, eds., *Introduction to Frustrated Magnetism: Materials, Experiments, Theory*, Vol. 164 (Springer, New York, 2011).
- [40] H. T. Diep, ed., *Frustrated Spin Systems* (World Scientific, Singapore, 2013).
- [41] R. Moessner and A. P. Ramirez, Geometrical frustration, *Phys. Today* **59**, 24 (2006).
- [42] X. Zheng, D. Zeng, and F.-Y. Wang, Social balance in signed networks, *Inf. Syst. Front.* **17**, 1077 (2014).
- [43] E. Lieb and D. Mattis, Ordering energy levels of interacting spin systems, *J. Math. Phys.* **3**, 749 (1962).
- [44] L. Savary and L. Balents, Quantum spin liquids: a review, *Rep. Prog. Phys.* **80**, 016502 (2016).
- [45] Y. Zhou, K. Kanoda, and T.-K. Ng, Quantum spin liquid states, *Rev. Mod. Phys.* **89**, 025003 (2017).
- [46] T. Lancaster, Quantum spin liquids, *arXiv:2310.19577* (2023).
- [47] U. Schollwöck, The density-matrix renormalization group in the age of matrix product states, *Ann. Phys.* **326**, 96 (2011).
- [48] M. Fishman, S. White, and E. Stoudenmire, The ITensor software library for tensor network calculations, *SciPost Phys. Codebases*, 4 (2022).
- [49] See Supplemental Material, which includes Refs. [82, 83], for statistics of the total spin on random trees, random regular graphs, scale-free graphs with tunable assortativity, comparison with classical spins, and exact solutions for the wheel for classical and quantum spins.
- [50] S. Aref and M. C. Wilson, Measuring partial balance in signed networks, *J. Complex Netw.* **6**, 566 (2017).
- [51] P. Holme, F. Liljeros, C. R. Edling, and B. J. Kim, Network bipartivity, *Phys. Rev. E* **68**, 056107 (2003).
- [52] S. Aref and M. C. Wilson, Balance and frustration in signed networks, *J. Complex Netw.* **7**, 163 (2018).
- [53] G. Caldarelli, *Scale-Free Networks: Complex Webs in Nature and Technology* (Oxford University Press, Oxford, UK, 2007).
- [54] A.-L. Barabási and R. Albert, Emergence of scaling in random networks, *science* **286**, 509 (1999).
- [55] N. C. Wormald, The asymptotic distribution of short cycles in random regular graphs, *J. Comb. Theory, Ser. B* **31**, 168 (1981).
- [56] H. Bonneau, A. Hassid, O. Biham, R. Kühn, and E. Katzav, Distribution of shortest cycle lengths in random networks, *Phys. Rev. E* **96**, 062307 (2017).
- [57] M. Bayati, A. Montanari, and A. Saberi, Generating random networks without short cycles, *Oper. Res.* **66**, 1227 (2018).
- [58] P. Holme and B. J. Kim, Growing scale-free networks with tunable clustering, *Phys. Rev. E* **65**, 026107 (2002).
- [59] P. Van Mieghem, H. Wang, X. Ge, S. Tang, and F. A. Kuipers, Influence of assortativity and degree-preserving rewiring on the spectra of networks, *Eur. Phys. J. B* **76**, 643 (2010).
- [60] R. Xulvi-Brunet and I. M. Sokolov, Changing correlations in networks: assortativity and disassortativity, *Acta Phys. Pol. B* **36**, 1431 (2005).
- [61] R. Noldus and P. Van Mieghem, Assortativity in complex networks, *J. Complex Netw.* **3**, 507 (2015).
- [62] J. M. Kleinberg, R. Kumar, P. Raghavan, S. Rajagopalan, and A. S. Tomkins, The web as a graph: Measurements, models, and methods, in *Computing and Combinatorics*, Lecture Notes in Computer Science, Vol. 1627 (Springer, Berlin, 1999) pp. 1–17.
- [63] R. Kumar, P. Raghavan, S. Rajagopalan, D. Sivakumar, A. Tomkins, and E. Upfal, Stochastic models for the web graph, in *Proceedings of the 41st IEEE Annual Symposium on Foundations of Computer Science* (IEEE Computing Society, California, 2000) pp. 57–65.
- [64] M. Alam, K. S. Perumalla, and P. Sanders, Novel parallel algorithms for fast multi-GPU-based generation of massive scale-free networks, *Data Sci. Eng.* **4**, 61 (2019).
- [65] M. Karbach, K. Hu, and G. Müller, Introduction to the Bethe Ansatz II, *Comput. Phys.* **12**, 565 (1998).

- [66] M. Karbach and K.-H. Mutter, The antiferromagnetic spin-1/2-XXZ model on rings with an odd number of sites, *J. Phys. A* **28**, 4469 (1995).
- [67] A. Kay and D. G. Angelakis, Reproducing spin lattice models in strongly coupled atom-cavity systems, *Europhys. Lett.* **84**, 20001 (2008).
- [68] G. Bianconi, Enhancement of T_c in the superconductor-insulator phase transition on scale-free networks, *J. Stat. Mech.* **2012**, P07021 (2012).
- [69] G. Bianconi, Superconductor-insulator transition on annealed complex networks, *Phys. Rev. E* **85**, 061113 (2012).
- [70] G. Bianconi, Superconductor-insulator transition in a network of 2d percolation clusters, *Europhys. Lett.* **101**, 26003 (2013).
- [71] F. A. Rodrigues, T. K. D. Peron, P. Ji, and J. Kurths, The Kuramoto model in complex networks, *Phys. Rep.* **610**, 1 (2016).
- [72] H. Tasaki, From Nagaoka's ferromagnetism to flat-band ferromagnetism and beyond: An introduction to ferromagnetism in the Hubbard model, *Prog. Theor. Phys.* **99**, 489 (1998).
- [73] K.-S. Kim, Exact hole-induced resonating-valence-bond ground state in certain $U = \infty$ Hubbard models, *Phys. Rev. B* **107**, L140401 (2023).
- [74] C. P. Herrero, Antiferromagnetic Ising model in small-world networks, *Phys. Rev. E* **77**, 041102 (2008).
- [75] M. Bartolozzi, T. Surungan, D. B. Leinweber, and A. G. Williams, Spin-glass behavior of the antiferromagnetic Ising model on a scale-free network, *Phys. Rev. B* **73**, 224419 (2006).
- [76] C. P. Herrero, Antiferromagnetic Ising model in scale-free networks, *Eur. Phys. J. B* **70**, 435 (2009).
- [77] L. Balents, Spin liquids in frustrated magnets, *Nature (London)* **464**, 199 (2010).
- [78] R. Milo, S. Shen-Orr, S. Itzkovitz, N. Kashtan, D. Chklovskii, and U. Alon, Network motifs: Simple building blocks of complex networks, *Science* **298**, 824 (2002).
- [79] A. Silveira, R. Erichsen, and S. G. Magalhães, Geometrical frustration and cluster spin glass with random graphs, *Phys. Rev. E* **103**, 052110 (2021).
- [80] M. Morgado and S. Whitlock, Quantum simulation and computing with Rydberg-interacting qubits, *AVS Quantum Sci.* **3**, 023501 (2021).
- [81] P. Scholl, H. J. Williams, G. Bornet, F. Wallner, D. Barredo, L. Henriot, A. Signoles, C. Hainaut, T. Franz, S. Geier, A. Tebben, A. Salzinger, G. Zürn, T. Lahaye, M. Weidemüller, and A. Browaeys, Microwave engineering of programmable XXZ Hamiltonians in arrays of Rydberg atoms, *PRX Quantum* **3**, 020303 (2022).
- [82] M. Blume, P. Heller, and N. A. Lurie, Classical one-dimensional Heisenberg magnet in an applied field, *Phys. Rev. B.* **11**, 4483 (1975).
- [83] K. Bärwinkel, H.-J. Schmidt, and J. Schnack, Ground-state properties of antiferromagnetic Heisenberg spin rings, *J. Magn. Magn. Mater.* **220**, 227 (2000).

Supplemental Material for “Frustrated Quantum Magnetism on Complex Networks: What Sets the Total Spin”

I. Random trees

A tree has a bipartite structure [Fig. S1(a)], for which $S_{\text{total}} = |N_A - N_B|/2$, where N_A and N_B are the numbers of spins in the two sublattices. Figure S1(b) shows that both the average and the spread of S_{total} over random trees with N sites and $N - 1$ bonds scale as \sqrt{N} .

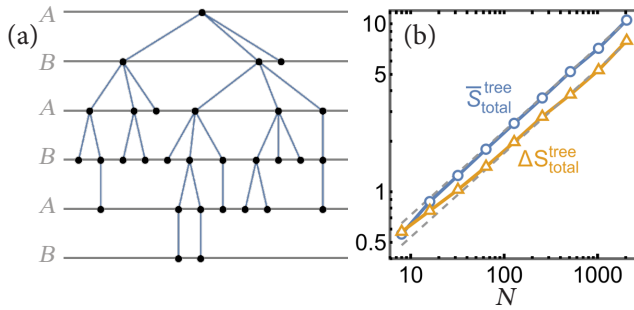


FIG. S1. (a) Tree with $N = 30$ sites. Horizontal lines show the two sublattices. (b) The average and the standard deviation of S_{total} over $\mathcal{N} = 1000$ random trees as a function of N . Dashed lines show the fits $0.23\sqrt{N}$ and $0.17\sqrt{N}$, respectively.

II. Random regular graphs

In the main text we showed that a random regular graph, where each node has $k = 3$ neighbors, almost always has $S_{\text{total}} = 0$. Figure S2 shows the same holds for $k = 4$ and $k = 5$, further demonstrating that heterogeneity is essential for nonzero total spin.

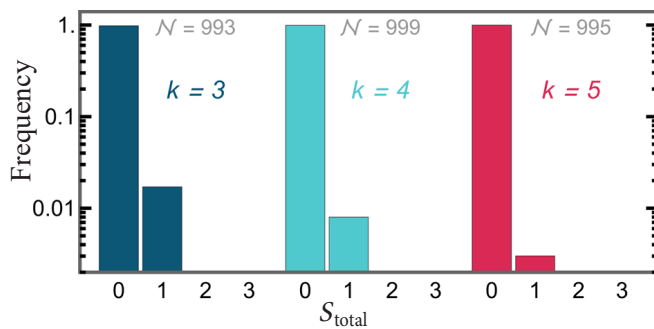


FIG. S2. Total-spin distribution of random regular networks with $N = 30$ sites for different values of the degree k .

III. Small-world networks

One can interpolate between a regular lattice and random graphs by randomly rewiring a small fraction of the bonds of the lattice; These “shortcuts” dramatically shorten the average path length between two nodes while maintaining a high clustering, resulting in a small-world character [S1]. Figure S3 shows that this procedure leads to a slow increase of the average total spin, which is accompanied by a similar rise in the heterogeneity. Thus, we find no strong dependence of S_{total} on the path length.

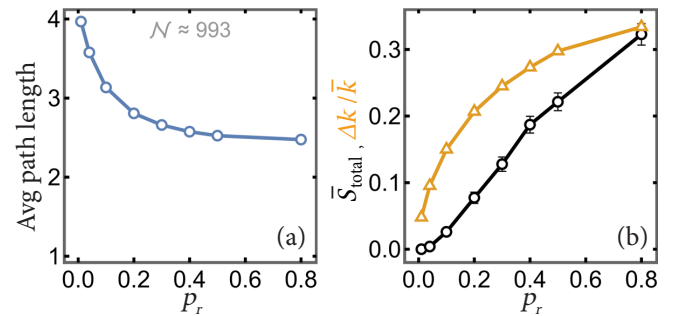


FIG. S3. (a) Path length, (b) total spin and heterogeneity as a function of the rewiring probability p_r for Watts-Strogatz graphs with $N = 30$ and $k = 4$.

IV. (Dis)assortative scale-free networks

In the main text we explained how tuning the assortativity of random graphs strongly affects S_{total} , which falls sharply with the assortativity coefficient A [S2]. Figure S4 shows the same is true for Barabási-Albert graphs with scale-free degree distribution ($p_k \sim 1/k^3$).

V. Exact solution for the wheel

In the main text we proposed a wheel-shaped network where the total spin can be tuned by varying some of the bond strengths. The network consists of N_c central spins and N_b outer spins with the Hamiltonian

$$\hat{H} = \frac{J_c}{2} \hat{\mathbf{S}}_c^2 + J \hat{\mathbf{S}}_b \cdot \hat{\mathbf{S}}_c + J_b \sum_{n=1}^{N_b} \hat{\mathbf{S}}_n \cdot \hat{\mathbf{S}}_{n+1} \quad (\text{S1})$$

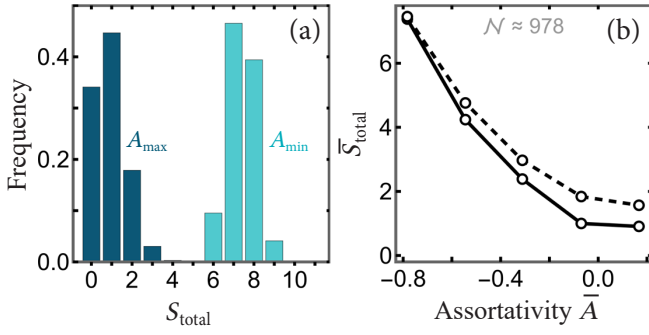


FIG. S4. (a) Total-spin distribution of the most assortative ($\bar{A} = +0.17$) and the most disassortative ($\bar{A} = -0.78$) scale-free graphs with $N = 30$ and $\bar{k} = 3.8$. (b) Variation of \hat{S}_{total} with the average assortativity. Dashed curve is for Ising spins.

up to a constant, where $\hat{\mathbf{S}}_c$ is the net central spin, $\hat{\mathbf{S}}_b := \sum_{i=1}^{N_b} \hat{\mathbf{S}}_i$ is the net outer spin, and $\hat{\mathbf{S}}_{N_b+1} \equiv \hat{\mathbf{S}}_1$. Below we describe exact solutions for the ground states of this network for both classical and quantum spins.

A. Classical spins

In order to lower energy \mathbf{S}_b and \mathbf{S}_c point in opposite directions. Without loss of generality we take \mathbf{S}_b along $+z$ and \mathbf{S}_c along $-z$. The maximum magnitude of \mathbf{S}_c is $N_c S$, where S is the magnitude of each spin. To compare with qubits we set $S = 1/2$ and write $\mathbf{S}_c = -(N_c/2)u\hat{z}$, where $u \in [0, 1]$. This central spin acts as an effective magnetic field for the Heisenberg ring [see Eq. (S1)], whose thermodynamic properties can be solved exactly [S3]. The field wants to polarize the spins along $+z$, whereas the bonds prefer a Néel-type antiferromagnet. In the ground state, the spins orient along the polar and azimuthal angles

$$\theta_n = \theta, \quad (\text{S2a})$$

$$\phi_n = n(\pi - \alpha) + \phi_0, \quad (\text{S2b})$$

where θ goes from 0 to $\pi/2$ as the field decreases, ϕ_0 is an arbitrary constant, and $\alpha = [1 - (-1)^{N_b}] \pi / (2N_b)$. Substituting these into the Hamiltonian gives the energy

$$\tilde{E} = \tilde{J}_c u^2 - 2uv + \tilde{J}_b \cos^2(\alpha/2) v^2, \quad (\text{S3})$$

where $v := \cos \theta$, $\tilde{E} := 8E / (JN_b N_c)$, $\tilde{J}_c := J_c N_c / (JN_b)$, and $\tilde{J}_b := 4J_b / (JN_c)$. Minimizing \tilde{E} with respect to the fractions u and v yields a ground state with $S_b = \frac{1}{2} N_b v$, $S_c = \frac{1}{2} N_c u$, and $S_{\text{total}} = \frac{1}{2} |N_b v - N_c u|$.

The resulting phase diagram comprises four regions:

$$u = v = 0 \quad \text{if } \tilde{J}_c \tilde{J}_b' > 1, \quad (\text{S4a})$$

$$u = v = 1 \quad \text{if } \tilde{J}_c < 1 \text{ and } \tilde{J}_b' < 1, \quad (\text{S4b})$$

$$u = 1, v = 1/\tilde{J}_b' \quad \text{if } \tilde{J}_c \tilde{J}_b' < 1 \text{ and } \tilde{J}_b' > 1, \quad (\text{S4c})$$

$$v = 1, u = 1/\tilde{J}_c \quad \text{if } \tilde{J}_c \tilde{J}_b' < 1 \text{ and } \tilde{J}_c > 1, \quad (\text{S4d})$$

with $\tilde{J}_b' := \tilde{J}_b \cos^2(\alpha/2)$, as shown in Fig. S5(a) for $N_b \gg N_c$. Note that $\alpha \approx 0$ for large N_b and the phase diagram does not depend on whether N_c is odd or even.

B. Quantum spins

Since $\hat{\mathbf{S}}_b^2$ and $\hat{\mathbf{S}}_c^2$ commute with \hat{H} and $S_{\text{total}} = S_{bc} := |S_b - S_c|$ in the ground state(s), we can write the lowest energy for a given S_b and S_c as

$$E = \frac{J_c}{2} \hat{S}_c^2 + \frac{J}{2} (\hat{S}_{bc}^2 - \hat{S}_b^2 - \hat{S}_c^2) + J_b E_b(N_b, S_b), \quad (\text{S5})$$

where $\hat{S}^2 := S(S+1)$ and E_b is the lowest energy of the Heisenberg ring. The latter can be found using the Bethe Ansatz [S4], which involves solving the equations

$$N_b \tan^{-1}(2\lambda_i) = \pi I_i + \sum_j \tan^{-1}(\lambda_i - \lambda_j) \quad (\text{S6})$$

for the rapidities λ_i , $i = 1, 2, \dots, N_\downarrow = N_b/2 - S_b$, where $I_i = i - (N_\downarrow + 1)/2$ for even N_b and $i - (N_\downarrow + 1 \pm 1)/2$ for odd N_b [S5], whereupon $E_b = N_b/4 - \sum_i 2/(4\lambda_i^2 + 1)$. The two sets of $\{I_i\}$ for odd N_b are degenerate in energy [S6]. The ground-state spins are obtained by minimizing E in Eq. (S5) over all quantum numbers $S_b = N_b/2, N_b/2 - 1, \dots$ and $S_c = N_c/2, N_c/2 - 1, \dots$.

Figures S5(b) and S5(c) show that the resulting phase diagram differs qualitatively for $N_c = 2$ and $N_c = 3$. As explained in the main text, this is because for odd N_c one cannot have $S_c = 0$, which leads to a stepwise fall of S_b as J_b is increased relative to J . To understand this feature more precisely we consider the energy as a function of S_b for a given $S_c < S_b$,

$$\tilde{E} = \text{constant} + \frac{4S_c}{N_c} f_\downarrow + \frac{\tilde{J}_b}{2} \tilde{E}_b(f_\downarrow), \quad (\text{S7})$$

where $f_\downarrow := 1 - 2S_b/N_b$ is twice the fraction of \downarrow spins in the ring, and $\tilde{E}_b := 4E_b/N_b$. For large S_b (small f_\downarrow) one can write $\tilde{E}_b \approx 1 - 4f_\downarrow + \eta f_\downarrow^3$, where $\eta \sim O(1)$ [Fig. S5(d)], which predicts the minimum energy for

$$f_\downarrow \approx [4(\tilde{J}_b - \tilde{J}_b^*) / (3\eta \tilde{J}_b)]^{1/2} \quad (\text{S8})$$

when $\tilde{J}_b > \tilde{J}_b^* := 2S_c/N_c$. Consequently, the susceptibility $\partial S_b / \partial \tilde{J}_b$ diverges as

$$\frac{\partial S_b}{\partial \tilde{J}_b} \approx -\frac{N_b}{2\sqrt{3\eta} \tilde{J}_b^*} \left(\frac{\tilde{J}_b}{\tilde{J}_b^*} - 1 \right)^{-1/2}, \quad (\text{S9})$$

which is seen in Fig. S5(b) for $S_c = 1$ and in Fig. S5(c) for $S_c = 3/2, 1/2$. No such divergence is present for classical spins [Fig. S5(a)].

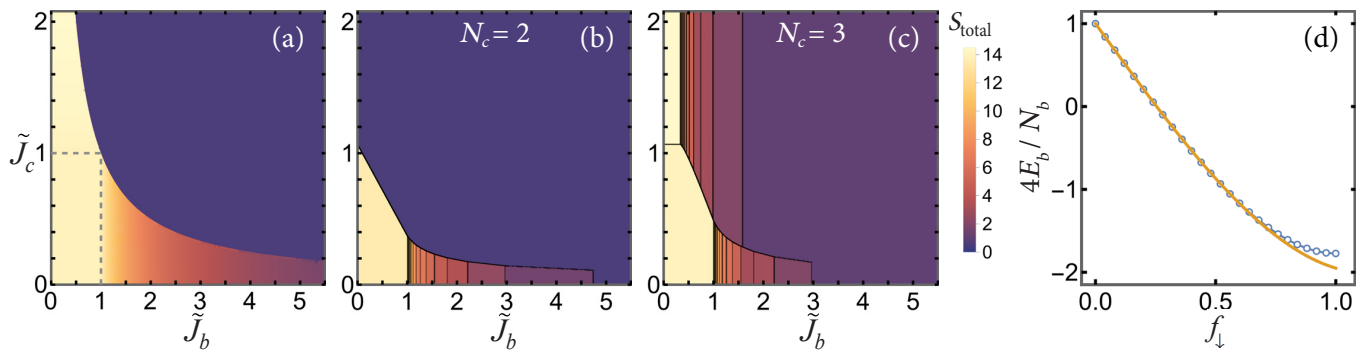


FIG. S5. Phase diagram of the wheel-shaped network introduced in the main text [Eq. (S1)] for (a) classical spins with $N_c = 2$, $N_b = 30$, (b) qubits with $N_c = 2$, $N_b = 30$, and (c) qubits with $N_c = 3$, $N_b = 30$. (d) Minimum energy of the Heisenberg ring as a function of twice the fraction of \downarrow spins for $N_b = 50$. Orange curve shows the fit $1 - 4f_\downarrow + 1.05f_\downarrow^3$.

VI. Quantum vs. classical S_{total}

Figure S6 shows a comparison between the total spins of classical and quantum Heisenberg models defined on two types of networks: (i) random graphs and (ii) graphs generated by the copy model introduced in the main text, where heterogeneity and assortativity can be tuned by varying a structure parameter p . Generally, we find that the two spins are highly correlated and that the classical total spin is larger by $O(1)$.

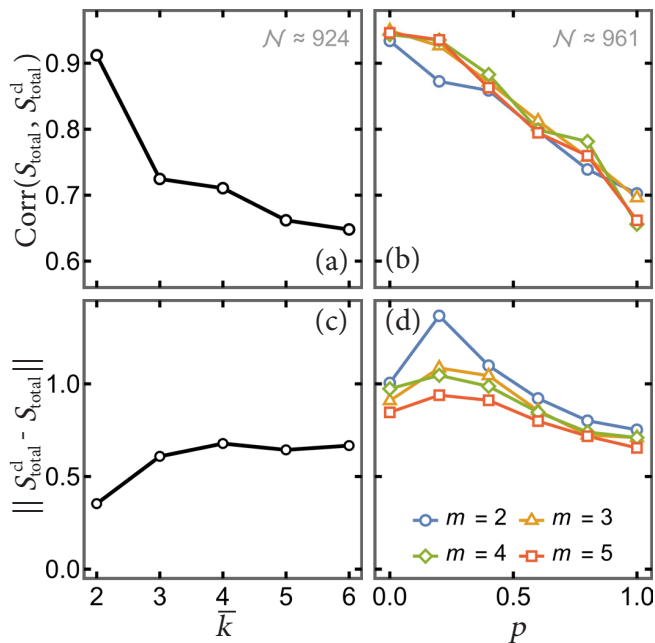


FIG. S6. (Top panel) Correlation and (bottom panel) root-mean-square deviation between the net magnetizations of classical and quantum spins for random graphs (left column) and graphs generated by the growth model introduced in the main text (right column) with $N = 30$ sites.

- [S1] D. J. Watts and S. H. Strogatz, Collective dynamics of ‘small-world’ networks, *Nature (London)* **393**, 440 (1998).
- [S2] M. E. J. Newman, Assortative mixing in networks, *Phys. Rev. Lett.* **89**, 208701 (2002).
- [S3] M. Blume, P. Heller, and N. A. Lurie, Classical one-dimensional Heisenberg magnet in an applied field, *Phys. Rev. B.* **11**, 4483 (1975).
- [S4] M. Karbach, K. Hu, and G. Müller, Introduction to the Bethe Ansatz II, *Comput. Phys.* **12**, 565 (1998).
- [S5] M. Karbach and K.-H. Mutter, The antiferromagnetic spin-1/2 -XXZ model on rings with an odd number of sites, *J. Phys. A* **28**, 4469 (1995).
- [S6] K. Bärwinkel, H.-J. Schmidt, and J. Schnack, Ground-state properties of antiferromagnetic Heisenberg spin rings, *J. Magn. Magn. Mater.* **220**, 227 (2000).